Available online at www.sciencedirect.com
ScienceDirect
ELSEVIER
International Journal of Rock Mechanics & Mining Sciences 44 (2007) 321–331
International Journal of Rock Mechanics and Mining Sciences
www.elsevier.com/locate/ijrmms

Influence of surrounding environments and strain rates on the strength of rocks subjected to uniaxial compression

Hae-sik Jeong[a], Seong-seung Kang[b], Yuzo Obara[c,*]

[a]Geomax Co. Ltd., Korea
[b]Research Institute of Basic Sciences, Sunchon National University, Korea
[c]Department of Civil Engineering, Kumamoto University, Japan

Accepted 3 July 2006
Available online 29 September 2006

Abstract

Uniaxial compression tests were performed under various non-atmospheric environments and constant strain rates on Kumamoto andesite. The environments considered were water vapor, organic vapor such as methanol, ethanol and acetone, and inorganic gas such as argon, nitrogen and oxygen. The strength of rock increased in the order of water vapor, methanol, ethanol and acetone vapor, and the stress corrosion index changed with changing environment even for the same rock type. The stress corrosion index was evaluated to be 31 in consideration of the water vapor pressure and strain rate. The stress corrosion index in this research showed good agreement with other researchers' results and it can be concluded that the stress corrosion index is one of the constants representing the mechanical properties of the rock. However, it is an environment-dependent factor and may vary owing to the difference of hydroxyl ion concentrations that may exist in the same rock. Finally, it was shown that the time to failure is delayed by decreasing water vapor pressure in the surrounding environment, and then the long-term strength of rock under water vapor pressure can be estimated, based on sub-critical crack growth due to stress corrosion.

Keywords: Rock; Uniaxial compression test; Non-atmospheric environment; Stress corrosion index; Long-term strength

1. Introduction

In completely brittle elastic materials, a crack is in a stable state for a stress intensity less than the critical stress intensity factor, the latter being known as the fracture toughness; however, the crack becomes unstable when the stress intensity factor reaches a critical value and it begins to propagate rapidly [1]. The critical value of the associated rock strength is largely dependent on mineralogical properties such as the compositions and textures of the minerals, and the quantity, shape and orientation of pre-existing cracks in the rock.

Under certain environmental conditions, especially high temperature and/or reactive environments, delayed failures dependent on the time for crack growth are observed for most materials when a static load below critical stress intensity factor is applied [2]. This phenomenon known as sub-critical crack growth, depends on several possible mechanisms, such as stress corrosion, dissolution, diffusion, ion-exchange and microplasticity [3]. Among them, stress corrosion is the main mechanism behind sub-critical crack growth in shallow crustal conditions, i.e. for the upper 20 km of the earth's crust [4,5].

First observed in 1899 by Grenet using glasses, stress corrosion has been reported in ceramics [6–9] and minerals and rocks [10–13]. Stress corrosion cracking was originally defined as environmentally induced sub-critical crack growth under static stress [14]. Recently, this definition has been extended to include mechanical failure, such as crack growth due to fatigue and creep stress in the absence of chemical phenomena. Therefore, stress corrosion has to be understood not only in terms of the chemical parameters of the surrounding environment but also in terms of the mechanical factors. However, there are few experiments to clarify the effect of a rock's surrounding environment on its

*Corresponding author. Tel./fax: +81 96 342 3686.
E-mail address: obara@kumamoto-u.ac.jp (Y. Obara).

1365-1609/$ - see front matter © 2006 Elsevier Ltd. All rights reserved.
doi:10.1016/j.ijrmms.2006.07.009

mechanical properties and strength. In this research, the influence of the surrounding environment and strain rate on the strength of rock is experimentally investigated.

The study of the long-term strength of rock is necessary for examining the stability of underground openings, such as caverns, for hydraulic power plant and nuclear waste disposal constructed underground, bearing in mind that the rock mass around an underground opening is generally in a high humidity state due to the presence of groundwater. Since water is considered to be the most effective agent to promote stress corrosion of rock [5], stress corrosion should be considered in estimating the long-term strength of rock in the water, or under a water vapor environment. However, there have been few experiments to investigate the influence of the water vapor environment on rock strength.

To rectify this situation, uniaxial compression tests were firstly performed under various environments (different from atmospheric) on Kumamoto andesite. The environments used in these tests were water vapor, organic vapor, such as methanol, ethanol and acetone, and inorganic gas such as argon, nitrogen and oxygen. The purpose was to establish whether water is the most effective agent in promoting stress corrosion of rock. Secondly, a series of uniaxial compression test was conducted under various water vapor pressures and strain rates. By analyzing the mechanical behavior and the strength of the rock specimens, the influence of water vapor pressure and strain rate on stress corrosion can be clarified. Furthermore, the stress corrosion index from the experiment can be compared with those of other researchers. Finally, the long-term strength of rock can be discussed, based on a theory and experimental results obtained in this research.

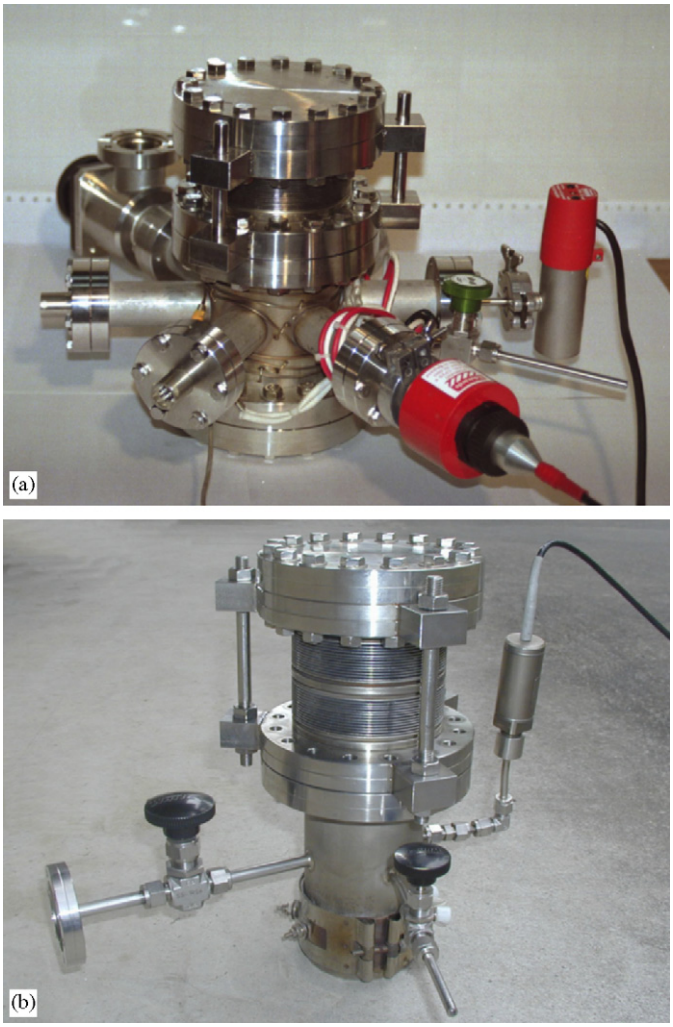

Fig. 1. Photograph of vacuum chambers: (a) chamber A for low pressure; (b) chamber B for high pressure.

2. Experimental apparatus and specimen

In order to control the surrounding environment of a sample rock, two chambers were made as shown in Fig. 1: chamber A is used for pressures below 2×10^3 Pa and room temperature; chamber B is used for high pressures and high temperature below 200 °C. chamber A, which was made of SUS304, has six ports and a valve to inject gases. In these ports, two ports were used to lead the output from the strain gauges glued to the specimen surface. Two other ports measured the vapor pressure in the chamber by two pressure gauges, namely the Pirani and Penning pressure gauges, which had a measurement range of 10^5–10^{-1} and 10^0–10^{-6} Pa, respectively. One port was the window for observing inside the chamber, and the other port with a valve was used to evacuate the air in the chamber by vacuum pumps.

Chamber B had two ports, a gas injection valve and a heater that controlled the temperature on the surface of the chamber. In two ports, the pressure transducer and the evacuation valve were connected.

The evacuation valve was linked to the two vacuum pumps: one was a turbo-molecular pump for high vacuum, and the other was a rotary pump for low vacuum. The evacuation velocity of the former was 160 l/s (N_2), and the ultimate pressure was 10^{-7} Pa. For the latter, those parameters were 90 l/s (N_2) and 10^2 Pa, respectively.

Kumamoto andesite was used as the experimental rock in this research. This rock type is porphyritic, consisting of plagioclase (about 50%), hornblende and augite (2~3%) as phenocrysts in a fine-grained groundmass. Because Kumamoto andesite is isotropic and homogeneous [15], core was randomly drilled from a cubic block. The size of the specimens was 35 mm in diameter and 70 mm in length for uniaxial compression. The ends of the specimen were polished flat to 0.01 mm.

Because the purpose of the work is to clarify the influence of the surrounding environment on the mechanical behavior of rock, the water within a rock should initially be removed completely. For this purpose, the specimens were dried at 197 °C in the oven for about 80 days for the uniaxial compression tests. The changes of the longitudinal wave velocity V_P and unit weight γ of the specimen during drying are shown in Fig. 2. The vertical

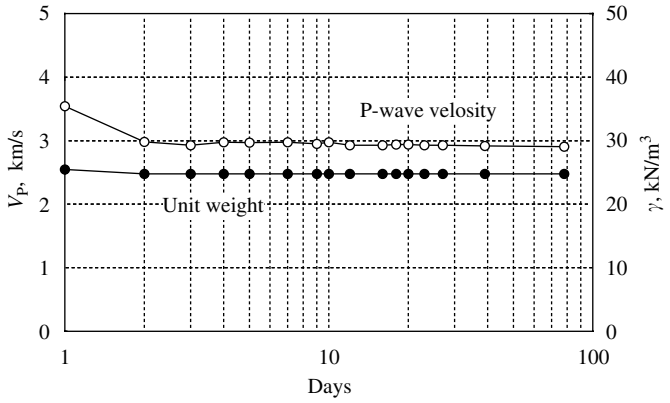

Fig. 2. Change of the longitudinal wave velocity and unit weight of the specimen during drying.

axis represents V_P and γ and the horizontal axis shows the elapsed time of drying on a log scale. V_P and γ of the specimen before drying are plotted for the first day. The V_P and γ were 2.9 km/s and 24.8 kN/m^3 after drying. The specimens were kept in a desiccator after drying.

A servo-controlled testing machine having a capacity of 500 kN was used for the uniaxial compression tests and the loading was controlled via a constant strain rate.

3. Influence of the surrounding environment

3.1. Experimental procedure

Thus, uniaxial compression tests on Kumamoto andesite in non-atmospheric environments were conducted to investigate the effect of surrounding environments on the strength of rock. The tests were performed at the constant pressure of the non-atmospheric environment in the chamber, 10^3 Pa, and at a constant strain rate using chamber A. The environments used in this research were methanol, ethanol and acetone as organic vapor, and argon, nitrogen, oxygen and hydrogen as inorganic gas and water vapor. A non-atmospheric environment can be produced by injecting a new vapor or gas environment after evacuating the air in the chamber. The cross section of the chamber A in which the specimens were set up is shown in Fig. 3. The upper and lower flanges each had a rod for applying compression. The load was transmitted to the specimen through the rods by compressing the flanges from the testing machine.

Fig. 4 shows an example of variation of the pressure in the chamber during testing. At first, the air was evacuated by two vacuum pumps. After that, water or organic material or gas was put in through the injection valve until the pressure of the chamber became the saturated pressure of water vapor at room temperature, 10^3 Pa. It was assumed that the air in the chamber can be fully changed to a new environment. Then the uniaxial compression test was performed after maintaining the new environment for about 6 h.

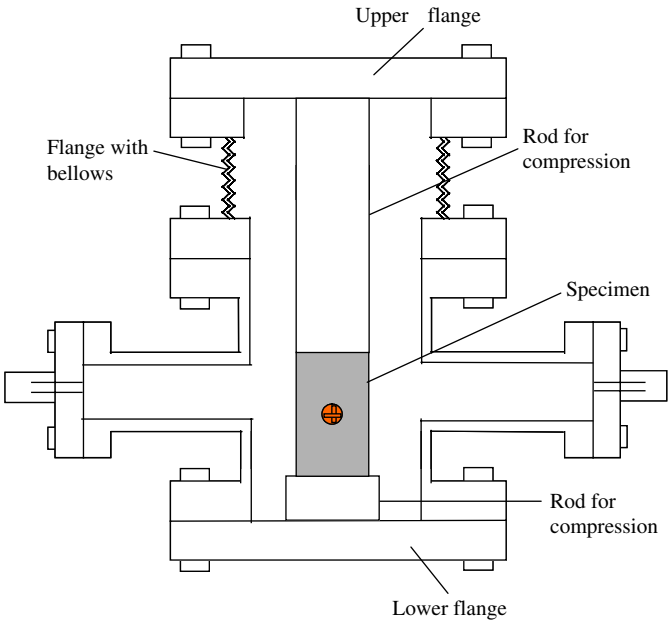

Fig. 3. Schematic diagram of the setup of the specimen in the chamber.

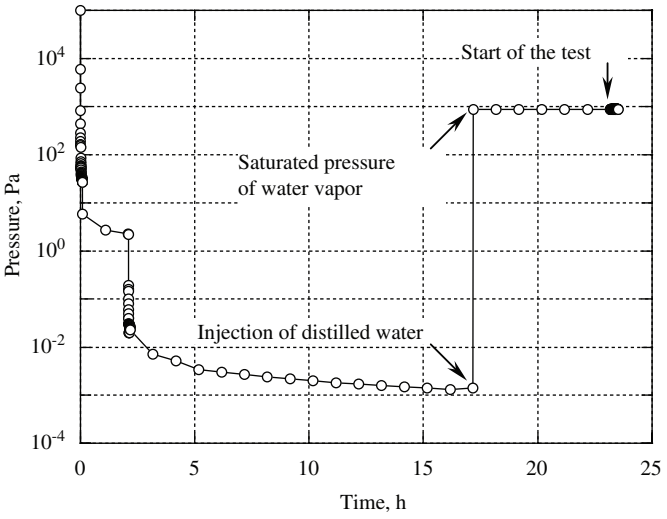

Fig. 4. Change of the pressure in the chamber during the test.

Note that the purpose of these tests was to investigate the influence of the surrounding environment on the strength of rock. However, it is difficult to permeate the surrounding gas into the rock in only 6 h under the condition of a pressure of 10^3 Pa—which value is smaller than that of atmospheric pressure—since the coefficient of air permeability of the rock is low. Therefore, the inside environment of the rock is considered to be different form the outside one. Consequently, the penetration of the surrounding gas into the rock is not considered in the tests.

4. Results

The testing conditions and results of the uniaxial compression test are listed in Table 1. The pressure in the chamber was 1.0×10^3 Pa and the strain rate was

Table 1
Testing conditions and results of uniaxial compression tests

No.	Strain rate (10^{-6}/s)	Strength (MPa)	E (GPa)	v	Environment
1	10.3	73.0	14.5	0.23	Water vapor
2	6.8	80.6	17.0	0.18	
3	14.1	83.8	16.8	0.24	Methanol vapor
4	13.5	85.2	16.8	0.19	
5	10.4	86.8	15.3	0.21	Ethanol vapor
6	13.4	96.6	17.9	0.18	
7	6.3	98.5	18.2	0.19	Acetone vapor
8	9.2	106.8	19.4	0.17	
9	6.3	128.6	19.7	0.18	Argon
10	6.8	132.7	21.3	0.16	
11	6.9	133.8	20.9	0.17	
12	6.3	113.2	16.9	0.14	Nitrogen
13	6.0	125.4	21.4	0.18	
14	6.0	137.3	22.7	0.17	
15	6.8	130.3	18.4	0.19	Oxygen
16	6.6	130.1	19.5	0.21	
17	5.6	132.1	19.3	0.17	

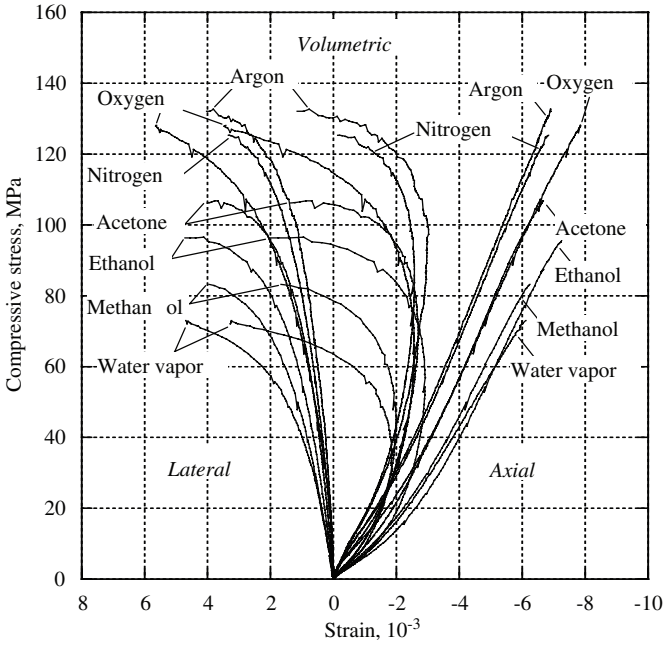

Fig. 5. Axial, lateral and volumetric strain curves of uniaxial compression test in each environment.

$5.6\sim13.5\times10^{-6}$/s during the experiments. The axial, lateral and volumetric strain curves for the uniaxial compression test under water vapor, organic vapor and inorganic gas environments are shown in Fig. 5. The stress–strain curves were only taken to the peak stress because there was no intention to monitor the post-failure effect. Two or three tests were conducted for each environment and the results for each environment are shown. The water vapor environment had the weakest strength, while the inorganic environment was the strongest. The Young's modulus was different in each environment.

Young's modulus E and Poisson's ratio v, which were measured at 50% of the ultimate strength in each environment, are plotted as shown in Fig. 6. The values of Young's modulus range between 15 and 23 GPa. However, Young's moduli in inorganic environments were higher than those in organic and water vapor environments. On the other hand, the Poisson's ratio was almost independent of the environments and was estimated to be 0.18.

The uniaxial compressive strength (UCS) S_c in each environment is shown in Fig. 7. The uniaxial compressive strength in the water vapor environment averaged 77 MPa. Those in methanol, ethanol and acetone were on average 85, 92 and 104 MPa, respectively. It is clear that the strength decreases in order of acetone, ethanol, methanol and water vapor. Note that the results for E and the UCS in Figs. 6 and 7 follow the same trend.

In the inorganic environments of argon, nitrogen and oxygen, the UCS was 129 MPa on average in spite of a scatter in the nitrogen results. It is considered that an inorganic environmental dependence on the strength does

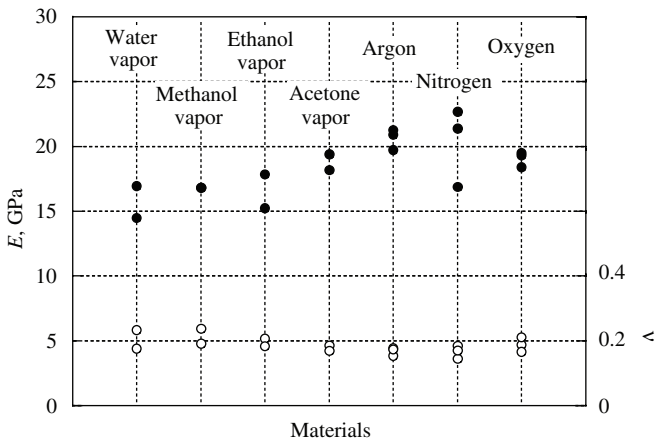

Fig. 6. Plot of Young's modulus and Poisson's ratio in each environment.

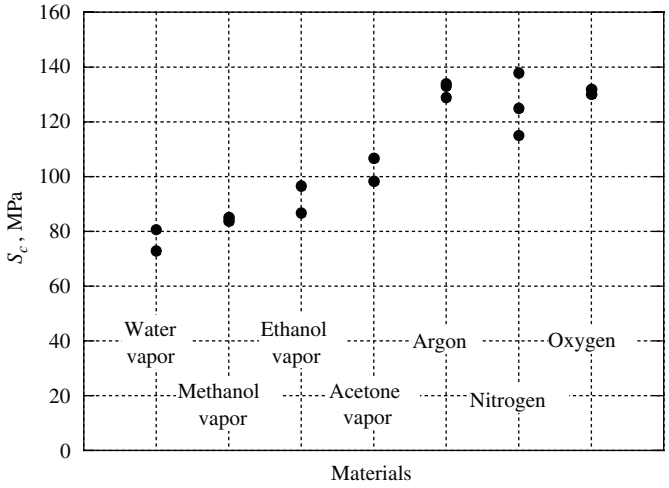

Fig. 7. Plot of uniaxial compressive strength in each environment.

not exist. These tendencies were similar to the plots of Young's modulus, and the UCS in water vapor environment was about 0.6 times of that in inorganic environments.

Thus, it is concluded that water influences the mechanical behavior of rock, in line with Atkinson and Meredith [5] who considered that water is the most effective agent in promoting stress corrosion in the sub-critical crack growth of rock. Therefore, the effect of water on the mechanical behavior of rock is further clarified in detail in the following section.

5. Stress corrosion and the strength of rock

Stress corrosion is the reaction between strained silicate minerals and environmental agents at the crack tip in rock, and is one of most important mechanisms of sub-critical crack growth. The surface energy of the crack tip drops due to stress corrosion so that the crack propagates more easily at a lower stress level. It is known that stress corrosion cracking occurs due to the characteristics of the surrounding environment, such as viscosity, pressure, temperature, humidity, pH etc [5,16–24]. Among these characteristics, the existence of water in the surrounding environment is closely related to the stress corrosion of rock. The action of stress corrosion is represented by the following equation [16,25,26]:

$$\mathrm{H-O-H+[\equiv Si-O-Si]\Leftrightarrow 2[\equiv Si-OH]}. \quad (1)$$

In order to express the sub-critical crack growth due to stress corrosion, two types of equation are used: namely, a power law and an exponential law [16,26]. These equations are suggested as the empirical relation between the crack velocity and tensile stress at the crack tip. Sano et al. [12] suggested use of the power law in order to analyze the relation between strength of rock and experimental parameters, such as stress and strain rate, water vapor pressure:

$$\mathrm{d}a/\mathrm{d}t = Ap^{n_w}\sigma^n, \quad (2)$$

where $\mathrm{d}a/\mathrm{d}t$ is the crack velocity, A a constant, p the water vapor pressure, n_w is the order of the rate-limiting chemical reaction and σ is the local tensile stress near the crack tip.

Using Eq. (2) and a statistical model of crack distribution within a rock, Sano et al. [12] and Sano [27] suggested the following relations:

$$\log S_c \propto \frac{n_w}{n+1}\log\left(\frac{\dot{\varepsilon}}{p}\right). \quad (3)$$

For p being constant,

$$\log S_c \propto \frac{1}{n+1}\log\dot{\varepsilon}. \quad (4)$$

For $\dot{\varepsilon}$ being constant,

$$\log S_c \propto -\frac{n_w}{n+1}\log p. \quad (5)$$

In these equations, n becomes a stress corrosion index when n_w is assumed to be equal to unity [28]. In this research, these equations are used for the subsequent analysis of experimental results.

6. Influence of water vapor pressure

6.1. Experimental procedure

A series of uniaxial compression tests on Kumamoto andesite was conducted under various water vapor pressures. The two vacuum chambers in Fig. 1 were used in the experiment. Fig. 8 shows the variation of the pressure in the chamber during the test with low pressure. After replacing the air with water vapor in the chamber, the water vapor was re-exhausted to the required value. This water vapor pressure was maintained for about 24 h, and then the uniaxial compression test was performed.

For the high pressure, in the first step, saturated vapor pressure at room temperature was established using the processes adopted for the low pressure. In that time, a little liquid water was created in the bottom of the chamber. Secondly, by applying heat with the heater attached to chamber B, a high vapor pressure was created by the evaporation of the water in the chamber. The vapor pressure was maintained for about 6 h. After that, the uniaxial compression test was performed. Since strain gages could not be glued on the specimen due to the high temperature, the strain of the specimen was obtained from the displacement of the actuator of the testing machine as follows: at first, the stiffness of the loading systems, namely the testing machine and the chamber, was obtained from the uniaxial compression test using a steel specimen. Then, the displacement of the rock specimen was estimated from the measured displacement of the actuator, and the axial strain was calculated by dividing the displacement by the specimen length.

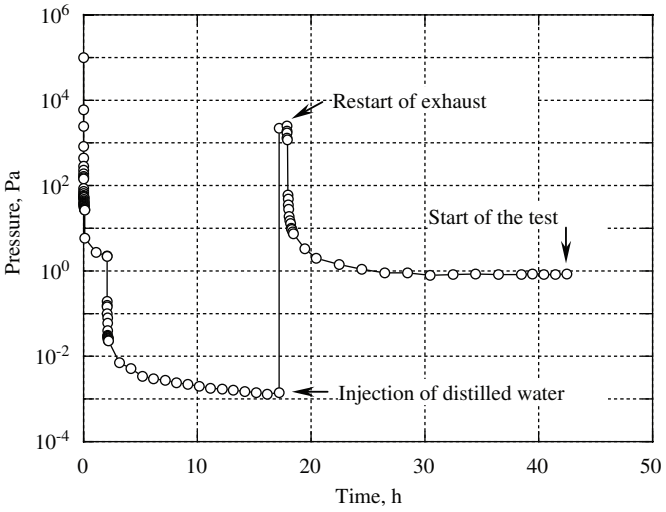

Fig. 8. Change of the pressure in the chamber during the test for low pressure.

6.2. Results

Because a heater was used to ensure a high water vapor pressure due to temperature, the influence of temperature on strength of rock had to be clarified before the tests. For this purpose, a series of uniaxial compression test was conducted on Kumamoto andesite using chamber B under atmospheric environment at various temperatures, namely, 23 (room temperature), 50, 100, 150 and 200 °C.

The stress–axial strain curves at each temperature are shown in Fig. 9. For the temperatures of 23 and 50 °C, failure occurred at the lower strain level. The strain level at failure increases with increasing temperature. The relation between the UCS S_c and Young's modulus E at each temperature is shown in Fig. 10. The results show that the increase in temperature up to 200 °C had only a small effect on the UCS and Young's modulus in this research. The reason is considered that the drying temperature of the specimen was 197 °C. Accordingly, it was concluded that the influence of temperatures 23–200 °C on the UCS and Young's modulus was negligible in these tests.

Uniaxial compression tests were conducted on Kumamoto andesite under various water vapor pressures. Firstly, the 16 specimens were tested totally in the water vapor environment. The pressure in the chamber was $5\times10^{-1}\sim10^{6}$ Pa and the strain rate varied from 0.68×10^{-6} to 10.3×10^{-6}/s. The testing conditions and results of the uniaxial compression test in the water vapor environment are shown in Table 2. The typical stress–axial strain curves are shown in Fig. 11. Those show straight lines generally except two curves. The UCS was relatively high in the case of the lower water vapor pressure.

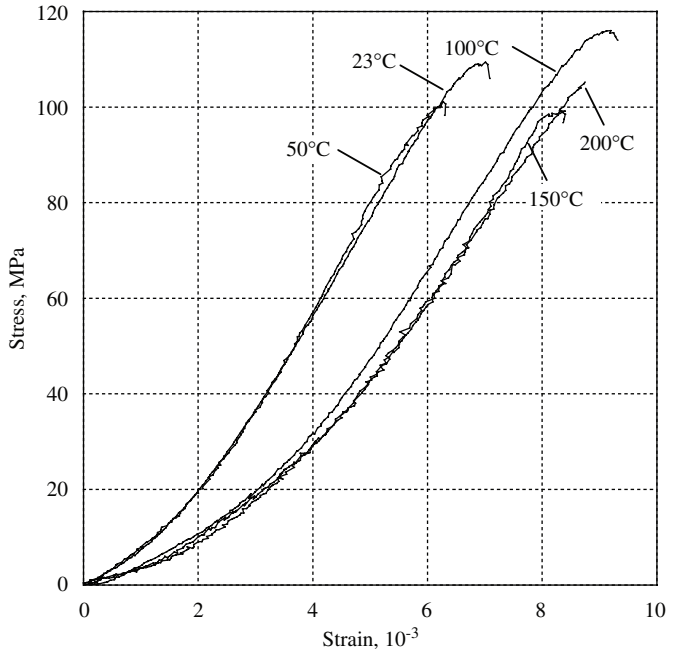

Fig. 9. Stress–axial strain curves of uniaxial compression test at various temperatures in the atmosphere.

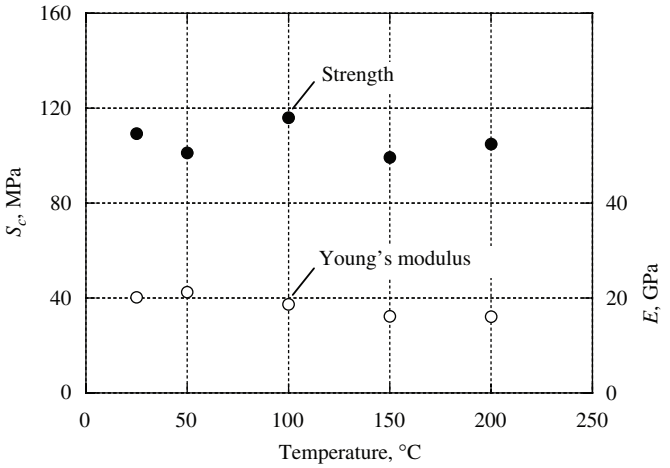

Fig. 10. Uniaxial compressive strength and Young's modulus at each temperature.

Table 2
Testing conditions and results of uniaxial compression tests in a water vapor environment

No.	Pressure (Pa)	Strain rate (10^{-6}/s)	Strength (MPa)	E (GPa)	Temperature (°C)	Failure type (see text)
1	1.1×10^{6}	5.8	52.5	16.8	184.2	II
2	1.0×10^{6}	6.5	60.3	15.9	180.1	I
3	9.9×10^{5}	7.2	51.7	12.7	179.6	II
4	3.4×10^{5}	6.1	63.9	17.6	138.0	I
5	1.6×10^{5}	7.2	65.2	16.0	113.5	I
6	1.7×10^{4}	5.2	65.3	20.8	56.7	II
7	7.6×10^{3}	9.6	75.4	16.9	40.7	I
8	1.4×10^{3}	0.68	80.6	17.0	23.0	I
9	1.3×10^{3}	10.3	73.0	14.5	23.0	II
10	1.7×10^{2}	1.8	78.2	13.8	23.0	II
11	1.0×10^{2}	2.4	88.9	14.6	23.0	I
12	2.6×10^{1}	1.9	91.9	15.1	23.0	I
13	9.0×10^{0}	1.2	83.8	13.3	23.0	II
14	6.0×10^{0}	1.6	85.3	15.2	23.0	II
15	1.0×10^{0}	1.0	91.7	18.2	23.0	II
16	5.0×10^{-1}	1.1	95.0	15.0	23.0	II

The failure mode of the Kumamoto andesite specimens was classified into two types: namely type I (failure with 1 or 2 shear planes); and type II (failure with tension failure and shear planes) as shown in Fig. 12. The failure type for each specimen is summarized in Table 2. A comparison of the strength of specimens conducted under almost the same water vapor pressure, i.e. specimens 8 and 9, showed that the strength of type II was about 11% less than that of type I. It is considered that the effective cross-sectional area was reduced owing to the progress of the exfoliation of the specimen and, as a result, the manifested strength was smaller.

Young's modulus E and UCS S_c were plotted with water vapor pressure as shown in Fig. 13. The Young's modulus appeared independent of water vapor pressure and its average value was 16 GPa. The strengths of the two failure types I and II are plotted as closed and opened circles,

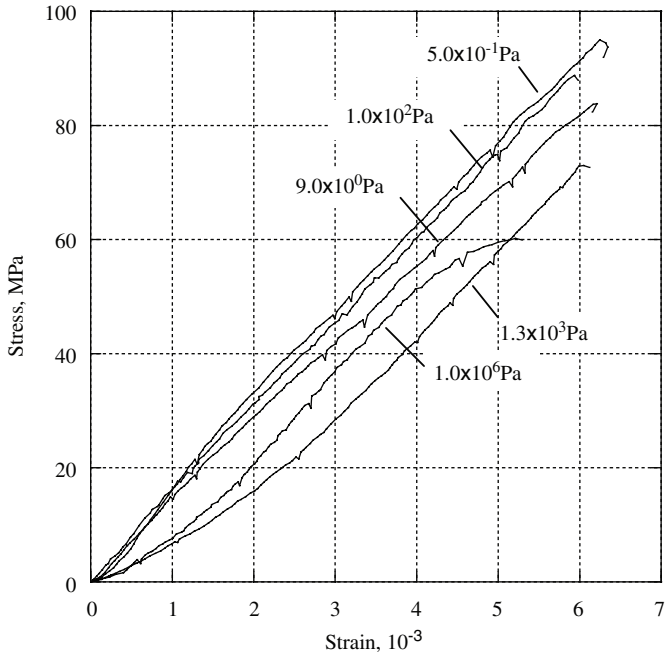

Fig. 11. Stress–axial strain curves of uniaxial compression test.

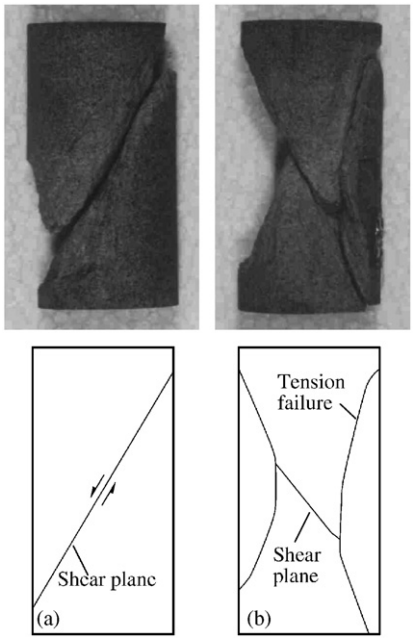

Fig. 12. Failure mode of the specimen for Kumamoto andesite: (a) failure with 1 or 2 shear planes and (b) failure with tension failure and shear planes.

respectively. It is clear that the UCS increases with decreasing water vapor pressure p. The slopes of the straight lines calculated by the least squares method were -0.04 in both types. This means that the effect of water vapor in the rock was similar, regardless of the type of failure. The UCS seemed to continue to increase with decreasing water vapor pressure. It is, however, considered

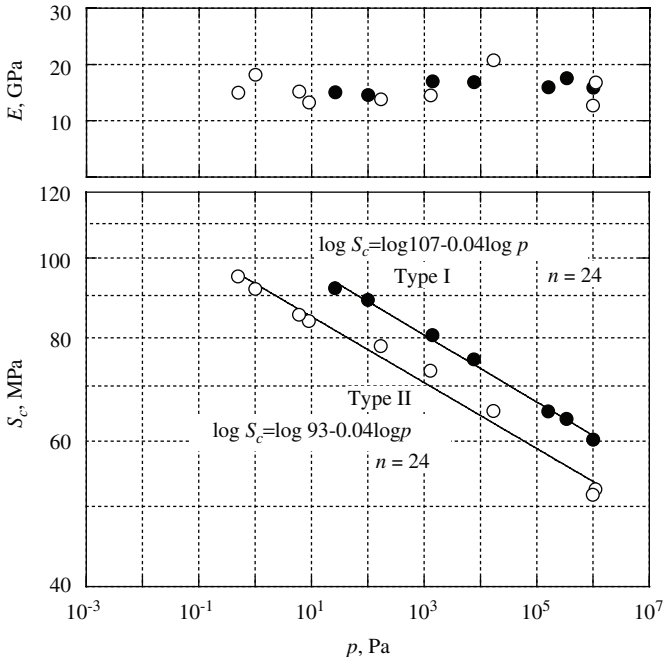

Fig. 13. Young's modulus and uniaxial compressive strength with the water vapor pressure. Closed and opened circles represent the results of failure types I and II, respectively.

that it will approach the UCS of intact rock under an anhydrous environment.

7. Influence of strain rate

7.1. Experimental procedure

In order to investigate the influence of the loading rate in the same environment, uniaxial compression tests were conducted in a water vapor environment. The tests were accomplished for three strain rate values: 181×10^{-6}, 18.7×10^{-6} and 1.23×10^{-6}/s. The control of water vapor pressure in the chamber was the same as used for the tests for the influence of vapor pressure. Three or four specimens were tested for each strain rate at different water vapor pressure levels.

7.2. Results

The testing conditions and results for the uniaxial compression test are shown in Table 3. The water vapor pressure ranged between 1.4×10^{-3} and 1.8×10^{3} Pa. The UCS increased with decreasing water vapor pressure. The Young's modulus and Poisson's ratio measured at a stress level of 50% of the strength are shown in Fig. 14. It was considered that, within the experimental parameters used here, Young's modulus and Poisson's ratio are not affected by strain rate, and that their mean values were 21.7 GPa and 0.31, respectively.

The influence of water vapor pressure p on UCS S_c in the case of the three strain rates is shown in Fig. 15, which has double logarithmic co-ordinates. The UCS increased

Table 3
Testing conditions and results of uniaxial compression tests for various water vapor pressures and strain rates

No.	Pressure, p (Pa)	Strain rate, $\dot{\varepsilon}$ (10^{-6}/s)	$\dot{\varepsilon}/p$ ($s^{-1}\,Pa^{-1}$)	Strength (MPa)	E (GPa)	v
1	9.4×10^{1}	1.62	1.72×10^{-8}	101.6	20.0	0.34
2	3.2×10^{-3}	1.12	3.50×10^{-4}	138.4	20.3	0.26
3	2.3×10^{-3}	0.95	4.13×10^{-4}	140.2	19.2	0.28
4	1.8×10^{3}	18.2	1.01×10^{-8}	107.2	20.6	0.26
5	3.0×10^{2}	19.2	6.40×10^{-8}	107.7	18.8	0.37
6	1.3×10^{-2}	18.6	1.43×10^{-3}	151.5	23.8	0.35
7	9.6×10^{2}	183	1.91×10^{-7}	116.5	21.5	0.26
8	2.1×10^{1}	172	8.19×10^{-6}	128.3	22.8	0.28
9	9.7×10^{-2}	179	1.85×10^{-3}	148.3	23.7	0.32
10	3.1×10^{-2}	191	6.16×10^{-3}	162.0	26.6	0.36

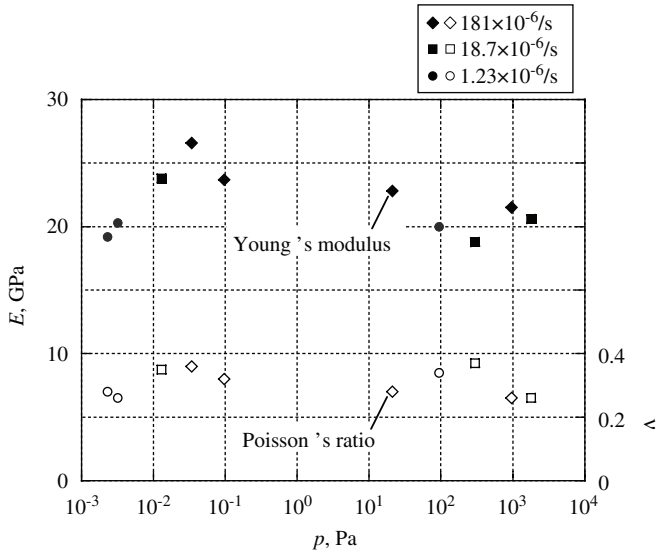

Fig. 14. Young's modulus (closed) and Poisson's ratio (opened) for each strain rate.

linearly with decreasing water vapor pressure for the same strain rate and with increasing strain rate. The slopes of the three lines obtained by least squares method for each strain rate were almost the same and corresponded to the term $-1/(n+1)$ in Eq. (5).

Thus, the stress corrosion index of Kumamoto andesite was not affected by strain rate in the range of this research. The average stress corrosion index can be estimated as 32 regardless of strain rate. Also the UCS increased with increasing strain rate for similar water vapor pressure and showed relatively high values for lower water vapor pressure.

The results regarding water vapor pressure and strain rate were replotted for the strength versus strain rate/water vapor pressure using double logarithmic co-ordinates, as shown in Fig. 16. In the figure, the horizontal axis represents the ratio of strain rate to water vapor pressure $\dot{\varepsilon}/p$. The UCS appears linearly proportional to $\dot{\varepsilon}/p$.

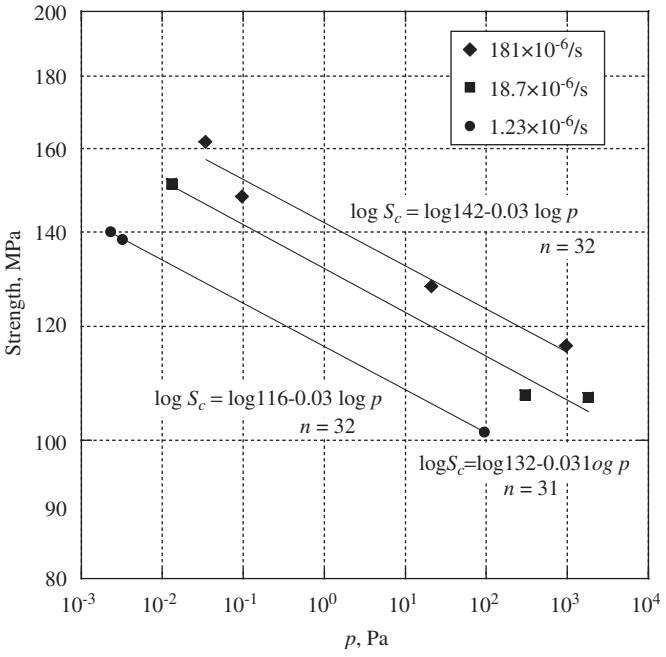

Fig. 15. Uniaxial compressive strength against water vapor pressure for each strain rate on the double logarithmic co-ordinates.

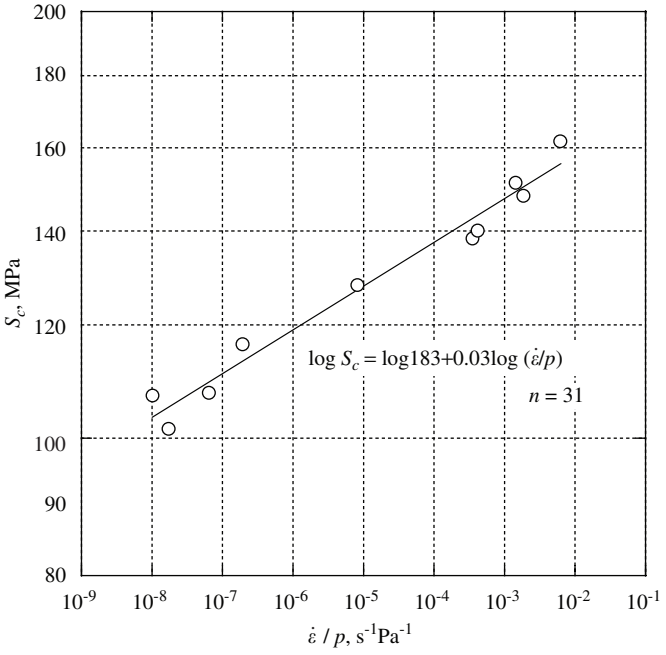

Fig. 16. Correlation of uniaxial compressive strength with the ratio of strain rate to water vapor pressure via double logarithmic co-ordinates.

A linear regression curve is also shown. The stress corrosion index calculated from Eq. (3) is estimated to be 31.

8. Discussion

Stress corrosion is the chemical reaction between hydroxyl groups and Si–O bonds at the crack tip. Therefore, it is clear that the stress corrosion cannot occur in an

inorganic environment, since there are no hydroxyl groups in inorganic gases.

The molecules of methanol and ethanol have hydroxyl groups. Silica is essentially insoluble in methanol and ethanol under standard conditions [29]. However, since the energy state at the crack tip is considered to be very high under loading, the reactions described by the following equations may take place in methanol and ethanol environments, respectively.

$$SiO_2 + 4CH_3OH \rightarrow Si(OCH_3)_4 + 2H_2O \quad (6)$$

and

$$SiO_2 + 4C_2H_5OH \rightarrow Si(OC_2H_5)_4 + 2H_2O. \quad (7)$$

In these reactions, water may be generated and used for the reaction of stress corrosion represented by the reaction (1). Furthermore, the solubility of silica in ethanol has been reported to be lower than that in methanol at the same high temperature [28]. Therefore, the amount of water generated from the reaction in methanol environment may be more than that in ethanol. It is considered that the degree of stress corrosion in methanol was greater than that in the ethanol environment.

Wiederhorn [30] derived an equation for crack velocity related to the hydroxyl ion concentration $[OH^-]$ at the crack tip as follows:

$$da/dt = B[OH^-]^{n_w} \exp[-\Delta G/RT], \quad (8)$$

where da/dt is the crack velocity, B a experimentally determined constant, T the temperature, n_w the order of the rate-limiting chemical reaction with respect to OH^- and G is the change of free energy as the chemical reaction goes from the initial to the final state. According to Eq. (8), OH^- is one of the most important factors in sub-critical crack growth for stress corrosion in rock.

The reaction at the crack tip followed reaction (1) in the water vapor environment. On the other hand, in the organic vapor environment having the hydroxyl group such as in methanol and ethanol, the reactions of (6) or (7) may first occur, and subsequently (1). Assuming that the free energy level at the crack tip is the same in both environments, the crack velocity may be fastest in the water vapor environment and be slower in the methanol and ethanol environment. Because of that, the concentration of OH^- was the highest in the water vapor environment and decreased in the order of methanol and ethanol environments. Consequently, it was considered that the strength was the lowest in the water vapor environment, and highest in the inorganic environment. From these considerations, it is concluded that water is the most effective agent which promotes stress corrosion of rock among the materials used in this research.

Secondly, the stress corrosion index in the water vapor environment will be discussed as compared with the results from other researchers. The data in Figs. 13 and 16 were replotted together with the results for various other rocks from John [31], Sangha and Dhir [32], Peng [33] and Sano et al. [12] via double-logarithmic co-ordinates as shown in Fig. 17. The vertical axis represents the strength, and the horizontal axis the ratio of strain rate and water vapor pressure. The experimental environments of John [31], Sangha and Dhir [32] and Peng [33] were regarded as atmospheric so that the water vapor pressure was assumed accordingly. The water vapor pressure used by Sano et al. [12] was calculated from the temperature and relative humidity during testing. The power law dependence of strength on water vapor pressure appears clearly.

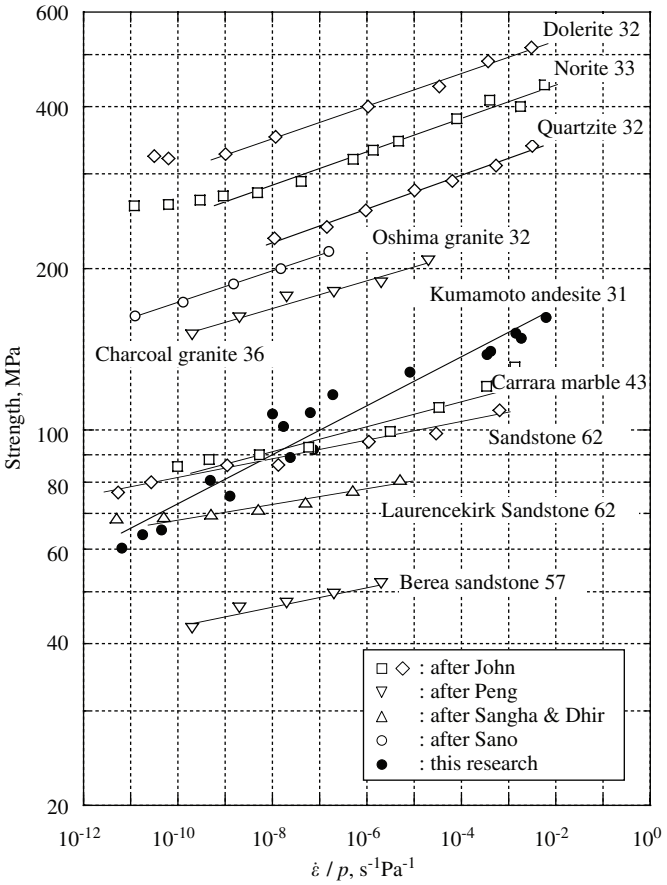

Fig. 17. Relations between the strength of rock and the ratio of strain/displacement rate and water vapor pressure, and comparison of stress corrosion indices of various rocks and minerals by John [31], Sangha and Dhir [32], Peng [33], and Sano et al. [12] with those in this paper (closed symbols).

The stress corrosion indices obtained from the slope of the linear regression curves are indicated in Fig. 17. According to this figure, the stress corrosion indices range from 32 to 62. The crystalline rocks, primarily composed of silicates minerals, seem to have a similar stress corrosion index—around 30. The stress corrosion index for Kumamoto andesite with varying water vapor pressure and strain rate was estimated from the uniaxial compression test to be 31 on average. The stress corrosion indices obtained in this research are in harmony with those of other researchers.

Also, Sano et al. [12] showed the influence of the partial pressure of water vapor on the UCS from the results of Charles [34], Krokosky and Husak [35] and Mizutani et al.

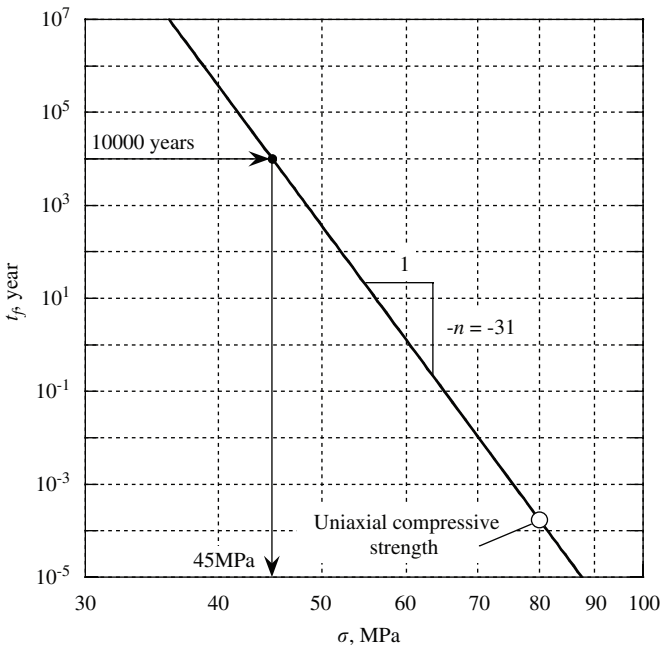

Fig. 18. Estimation of long-term strength of Kumamoto andesite, based on theory and stress corrosion index.

[36]. The stress corrosion index for Kumamoto andesite, commonly consisting of plagioclase, nearly coincides with that of albite. Compared with double torsion tests conducted by other researchers, the stress corrosion index for Kumamoto andesite is similar to the n value of 26 for Yugawara andesite, from Waza et al. [37].

Putting these results together, the stress corrosion indices obtained from the different testing methods or conditions are almost the same. Furthermore, they concur well with the results of other researchers. Consequently, it was concluded that the stress corrosion index could well be a constant for all rock types. It is almost constant regardless of testing methods, failure types and loading conditions. However, it is a factor that depends on the surrounding environment, and may vary in value owing to the difference in hydroxyl ion concentration present.

Finally, the long-term strength of rock is discussed based on our results because the rock mass around an underground opening is under a high humidity due to the groundwater. After completion of the opening, an induced stress is produced around it. Considering that this stress state may be unchanged in future, the stress state is regarded as time-dependent loading.

Sano [27] suggested the relation between the time to failure t_f and creep stress σ_0 as

$$\log t_f = -n \log \sigma_0 + B, \tag{9}$$

where n is the stress corrosion index and B a constant determined from a creep test. This equation corresponds to the results of other researchers [38–40].

According to this equation, the long-term strength can be estimated via Fig. 18. At first, the creep strength should be obtained from short-term creep tests. In order to simplify the discussion, however, it is assumed that the UCS is the creep strength and that the time consumed from start of loading to failure in the uniaxial compression test is the time to failure in a creep test. In this research, the UCS is 80 MPa on average at water vapor pressure of 10^{-3} Pa. The open circle is plotted as the UCS, and then the line can be drawn through the plot with a slope of $-n$. The value of the stress corrosion index of Kumamoto andesite is adopted to be 31 in consideration of the water vapor pressure and strain rate. From this procedure, the long-term strength after, for example, 10,000 years can be estimated as 45 MPa. This value is 56% of the short-term UCS.

Furthermore, the UCS of Kumamoto andesite can be increased to 1.1 times when the water vapor pressure is decreased to 0.1 times the saturated water vapor pressure at room temperature. Substituting this value for Eq. (9), the time to failure to the long-term strength of 45 MPa can be calculated as about 200,000 years, namely 20 times more. Consequently, it is important that the water vapor pressure in an underground opening is kept lower to ensure its stability for a longer time.

9. Conclusions

The influence of surrounding environments and strain rate on the strength of rock under various conditions using Kumamoto andesite was investigated. The stress corrosion index can be obtained from results of a series of uniaxial compression test under various vapor pressures and strain rates.

Firstly, a series of uniaxial compression test under various surrounding environments was performed. As a result, the environmental dependence on strength was found to be strongest for water vapor and it decreased in the order: acetone, ethanol, methanol and water vapor. However, the strength in inorganic environments was found to be independent of surrounding environments. This was considered to be caused by the difference in the hydroxyl ion concentration, which promotes sub-critical crack growth due to stress corrosion of the rock. It is concluded that water is the most effective agent to promote stress corrosion, which is significant because of the ubiquitous presence of groundwater around deep underground excavations.

Secondly, a series of uniaxial compression tests on Kumamoto andesite was conducted under various vapor pressures in order to clarify the effect of water vapor pressure on stress corrosion. The strength of rock in a water vapor environment increased as the water vapor pressure decreased and the strain rate increased. Furthermore, the stress corrosion index was not changed as the strain rate changed. From the observations, the stress corrosion index could be determined. The n value was evaluated to be 31 with consideration of the water vapor pressure and strain rate.

Compared with the results of other researchers, the stress corrosion index obtained in this research showed good agreement and, for a given rock, was found to be almost constant, regardless of testing methods, failure types and loading conditions. It can be concluded that the stress corrosion index is a material constant, representing one of the mechanical properties of a rock.

Finally, the long-term strength of Kumamoto andesite after 10,000 years can be estimated as 45 MPa, based on theory and the stress corrosion index obtained in the experiment. This value is 56% of the UCS value obtained in short-term tests. Furthermore, since the time to failure was found to be delayed by decreasing water vapor pressure in the surrounding environment, it is important that the water vapor pressure in an underground opening is kept at a low value to ensure the stability of an underground excavation for a longer time.

References

[1] Irwin GR. Fracture. In: Flügge S, editor. Handbuch der Physik, vol. 6. New York: Springer; 1958. p. 551–91.

[2] Stuart DA, Anderson OL. Dependence of ultimate strength of glass under constant load on temperature, ambient atmosphere and time. J Am Ceram Soc 1953;36:416–24.

[3] Atkinson BK. Subcritical crack growth in geological materials. J Geophys Res 1984;89:4077–114.

[4] Atkinson BK. Subcritical crack propagation in rocks: theory, experimental results and applications. J Struct Geol 1982;4:41–56.

[5] Atkinson BK, Meredith PG. The theory of subcritical crack growth with applications to minerals and rocks. In: Atkinson BK, editor. Fracture mechanics of rock. London: Academic Press; 1987. p. 111–66.

[6] Evans AG. A method for evaluating the time-dependent failure characteristics of brittle materials—and its application to ploycrystalline alumina. J Mater Sci 1972;7:1137–46.

[7] Wiederhorn SM. Fracture of ceramics, mechanical and thermal properties of ceramics. Spec. Publ. Nat Bur of Stand 1969;303:217–41.

[8] Wiederhorn SM. Subcritical crack growth in ceramics. In: Bradt RC, Hasselman DPH, Lange FF, editors. Fracture mechanics of ceramics, microstructure, materials, and applications, vol. 2. New York: Plenum; 1974. p. 613–46.

[9] Adams R, McMillan PW. Review: static fatigue in glass. J Mater Sci 1977;12:643–57.

[10] Scholz CH. Mechanism of creep in brittle rock. J Geophys Res 1968;73:3295–302.

[11] Wilkins BJS. Slow crack growth and delayed failure of granite. Int J Rock Mech Min Sci Geomech Abstr 1980;17:365–9.

[12] Sano O, Ito I, Terada M. Influence of strain rate on dilatancy and strength of Oshima granite under uniaxial compression. J Geophys Res 1981;86:9299–311.

[13] Atkinson BK, Meredith PG. Stress corrosion cracking of quartz: a note on the influence of chemical environment. Tectonophysics 1981;77:T1–T11.

[14] Speidel MO. Current understanding of stress corrosion crack growth in aluminum alloys. In: Scully JC, editor. The theory of stress corrosion cracking in alloys. Brussels: North Atlantic Treaty Organization; 1971. p. 289–344.

[15] Obara Y, Sakaguchi K, Nakayama T, Sugawara K. Anisotropy effect on fracture toughness of rock. In: Proceedings of ISRM Symposium: Eurock, vol. 92. 1992. p.7–12.

[16] Martin III RJ. Time-dependent crack growth in quartz and its application to the creep of rocks. J Geophys Res 1972;77:1406–19.

[17] Freiman SW. Effect of alcohols on crack propagation in glass. J Am Ceram Soc 1974;57:350–3.

[18] Wiederhorn SM, Johnson H. Effect of electrolyte pH on crack propagation in glass. J Am Ceram Soc 1973;56:192–7.

[19] Obara Y, Hirokawa H, Sugawara K. The strength of rocks under lower water vapor pressure. In: Proceedings of the 1st Korea–Japan joint symposium on rock engineering, 1996. p. 109–14.

[20] Obara Y, Sugawara K, Tokashiki N. Influence of water vapor pressure on strength of rocks under uniaxial compression. In: Proceedings of the 2nd North American rock mechanics symposium: NARMS, vol. 96. 1996. p. 1337–42.

[21] Obara Y, Jeong HS, Hirata A, Sato A, Sugawara K. Influence of surrounding environment on strength of rock under uniaxial compression. In: Proceedings of the international conference on geotechnology, geology engineering. Geo Eng 2000; CD-ROM:paper

[22] Jeong HS, Obara Y. Influence of surrounding environment on the strength of rock under Brazil test. In: Proceedings of the 3rd Korea–Japan joint symposium on rock engineering 2002. p. 139–44.

[23] Jeong HS, Obara Y. Strength of Kumamoto andesite in non-atmospheric environments (in Japanese). Shigen-to-Sozai 2002;118:599–604.

[24] Jeong HS, Obara Y, Sugawara K. The strength of rock under water vapor pressure (in Japanese). Shigen-to-Sozai 2003;119:9–16.

[25] Scholz CH. Static fatigue of quartz. J Geophys Res 1972;77:2104–14.

[26] Freiman SW. Effects of chemical environments on slow crack growth in glasses and ceramics. J Geophys Res 1984;89:4072–6.

[27] Sano O. Fundamental study on the mechanism of brittle fracture of rocks. PhD thesis, Kyoto University, Kyoto, Japan, 1978. p. 267.

[28] Wiederhorn SM. Fracture surface energy of glass. J Am Ceram Soc 1969;52:99–105.

[29] Iler RK. The chemistry of silica: solubility, polymerization, colloid and surface properties, and biochemistry. New York: Wiley-Interscience Publication; 1979.

[30] Wiederhorn SM. A chemical interpretation of static fatigue. J Am Ceram Soc 1972;55:81–5.

[31] John M. The influence of loading rate on mechanical properties and fracture processes of rock. CSIR Rep ME 1972:1115.

[32] Sangha CM, Dhir RK. Influence of time on the strength, deformation and fracture properties of a lower Devonian sandstone. Int J Rock Mech Min Sci Geomech Abstr 1972;9:343–54.

[33] Peng SS. Time-dependent aspects of rock behavior as measured by a servo-controlled hydraulic testing machine. Int J Rock Mech Min Sci Geomech Abstr 1973;10:235–46.

[34] Charles RJ. Static fatigue of glass. J Appl Phys 1958;29:1554–60.

[35] Krokosky EM, Husak A. Strength characteristics of basalt rock in ultra-high vacuum. J Geophys Res 1968;73:2237–47.

[36] Mizutani H, Spetzler H, Getting I, Martin III RJ, Soga N. The effect of outgassing upon the closure of cracks and the strength of lunar analogues. Proc Lunar Sci Conf 1977;8:1235–48.

[37] Waza T, Kurita K, Mizutani H. The effect of water on the subcritical crack growth in silicate rocks. Tectonophysics 1980;67:25–34.

[38] Cruden DM. The static fatigue of brittle rock under uniaxial compression. Int J Rock Mech Min Sci Geomech Abstr 1974;11:67–73.

[39] Schmidtke RH, Lajtai EZ. The long-term strength of Lac du Bonnet granite. Int J Rock Mech Min Sci Geomech Abstr 1985;22:461–5.

[40] Wilkins BJS. The long-term strength of plutonic rock. Int J Rock Mech Min Sci Geomech Abstr 1987;24:379–80.